

Electronic Structure of BiFeO₃ in Different Crystal Phases

J. KACZKOWSKI*, M. PUGACZOWA-MICHALSKA AND A. JEZIERSKI

Institute of Molecular Physics, Polish Academy of Sciences, M. Smoluchowskiego 17, 60-179 Poznań, Poland

The electronic structure of different phases of BiFeO₃ were calculated by using density functional theory. The DFT+*U* and semilocal Tran–Blaha modified Becke–Johnson potential were used. DFT+*U* results are in good agreement with previous calculations. Our results have shown that in case of *R3c*, *Pnma*, *Pn2₁a* BiFeO₃ has G-antiferromagnetic ordering and C-antiferromagnetic in case of *Cm* space group. In all calculated structures BiFeO₃ is a semiconductor with the band gap: 2.26 eV (2.27 eV) for *R3c*, 1.91 eV (1.66 eV) for *Pnma*, 1.99 eV (2.18 eV) for *Pn2₁a* and 2.09 eV (2.55 eV) for *Cm* within DFT+*U* (Tran–Blaha modified Becke–Johnson).

DOI: [10.12693/APhysPolA.127.266](https://doi.org/10.12693/APhysPolA.127.266)

PACS: 71.15.Mb, 77.84.–s, 75.85.+t, 75.47.Lx

1. Introduction

Bismuth ferrite (BiFeO₃) is the room-temperature multiferroic compound which have attracted an increasing interest due to its potential applications for magnetoelectric devices [1]. However the cycloid-type magnetic structure prevents the observation of the linear magnetoelectric effect [2, 3]. To overcome this problem and improve multiferroic properties, BiFeO₃ is doped with rare-earth (e.g. Y [4], Gd [5]) or transition metal (e.g. Ga [6]) atoms. Bulk BiFeO₃ has a rhombohedral symmetry (space group *R3c*) with *G*-type antiferromagnetic ordering, but doping leads to the structural phase transitions e.g. *R3c* → *Pn2₁a* → *Pnma* in case of Gd [5], *R3c* → *Pnma* for Y [4], and *R3c* → *Cm* for Ga [6]. The detailed study of the structural and electronic properties of different phases of BiFeO₃ have been presented in [7], where the extension of the density functional theory (DFT) known as DFT+*U* have been applied. DFT+*U* is based on the Hubbard model for strongly correlated electrons, where *U* is the on-site *d*–*d* Coulomb interaction [8]. In this paper we focus on the electronic structure of aforementioned phases of BiFeO₃ calculated within DFT+*U* and meta-generalized gradient approximation (meta-GGA) approaches. In the latter case we used the functional based on the formula proposed by Tran and Blaha which is modified version of the Becke–Johnson exchange potential (TB-mBJ) [9]. In general, in meta-GGA functionals the information from the kinetic energy density is used and the novel TB-mBJ functional provides a good agreement of band gap values for various semiconducting and insulating systems [10, 11]. The disadvantage of TB-mBJ is that it is not a functional derivative so cannot be use to calculate forces and geometry optimization [12].

In this paper the electronic structure of different phases of BiFeO₃ within both GGA+*U* and TB-mBJ potential will be presented. According to our knowledge there is no TB-mBJ calculations of electronic structures for these phases of BiFeO₃.

2. Method of calculations

The calculations were done by using the projector augmented wave method (PAW) [13] as implemented in Vienna ab initio Simulation Package (VASP) [14]. The Perdew–Burke–Ernzerhof (PBE) GGA [15] were used for exchange-correlation potential. The value of the *U* parameter in the DFT+*U* approach was *U*_{Fe} = 4 eV and was taken from [7]. The Brillouin zone integrations were performed by using 4 × 4 × 4 *Γ*-centered *k*-point grid. A kinetic energy cutoff of 520 eV and a total energy convergence threshold of 10^{−6} eV were used. The semicore *d* states were treated as core states in Bi. All the structures were fully relaxed within PBE+*U* approach and the obtained lattice constants and atomic coordinates were used for further studies of the electronic structure within semilocal TB-mBJ potential [9].

3. Results

The calculated crystallographic data were presented in one of our previous reports [16]. We compare the total energies among the *Cm*, *R3c*, *Pnma* and *Pn2₁a* crystal structures of BiFeO₃ together with the different spin arrangements (ferromagnetic and antiferromagnetic: A-, C- and G-AFM). The AFM spin arrangements of BiFeO₃

TABLE I

Calculated energy differences (meV/f.u.) between different phases of BiFeO₃ within PBE+*U* approach.

$\Delta E = E - E(R3c-G)$ [meV/f.u.]		
Space group	This work	[7]
<i>R3c-G</i>	0	0
<i>Pnma-G</i>	109	60
<i>Pn2₁a-G</i>	46	14
<i>Cm-C</i>	29	12

means that the spins on the Fe³⁺ ions are aligned in opposite senses. The ferromagnetic phase stacked antiferromagnetically on the *ab* planes in the *c*-axis for A-AFM. The antiferromagnetic phases stacked ferromagnetically on the *ab* plane in the *c* direction for C-AFM. The antiferromagnetic phase in three directions stacked

*corresponding author; e-mail: kaczkowski@ifmpan.poznan.pl

for G-AFM. The results are given in Table I. From the total energy calculations within PBE+ U the $R3c-G$ is the most stable phase. The G-AFM spin ordering is favorable in $Pnma$ and $Pn2_1a$ structures and C-AFM in Cm phase. Our results are in good agreement with previous

report [7]. The discrepancies in Table I between our results and previous results from [7] could be connected with the values of numerical parameters e.g. Gaussian smearing etc., but general the trend is preserved.

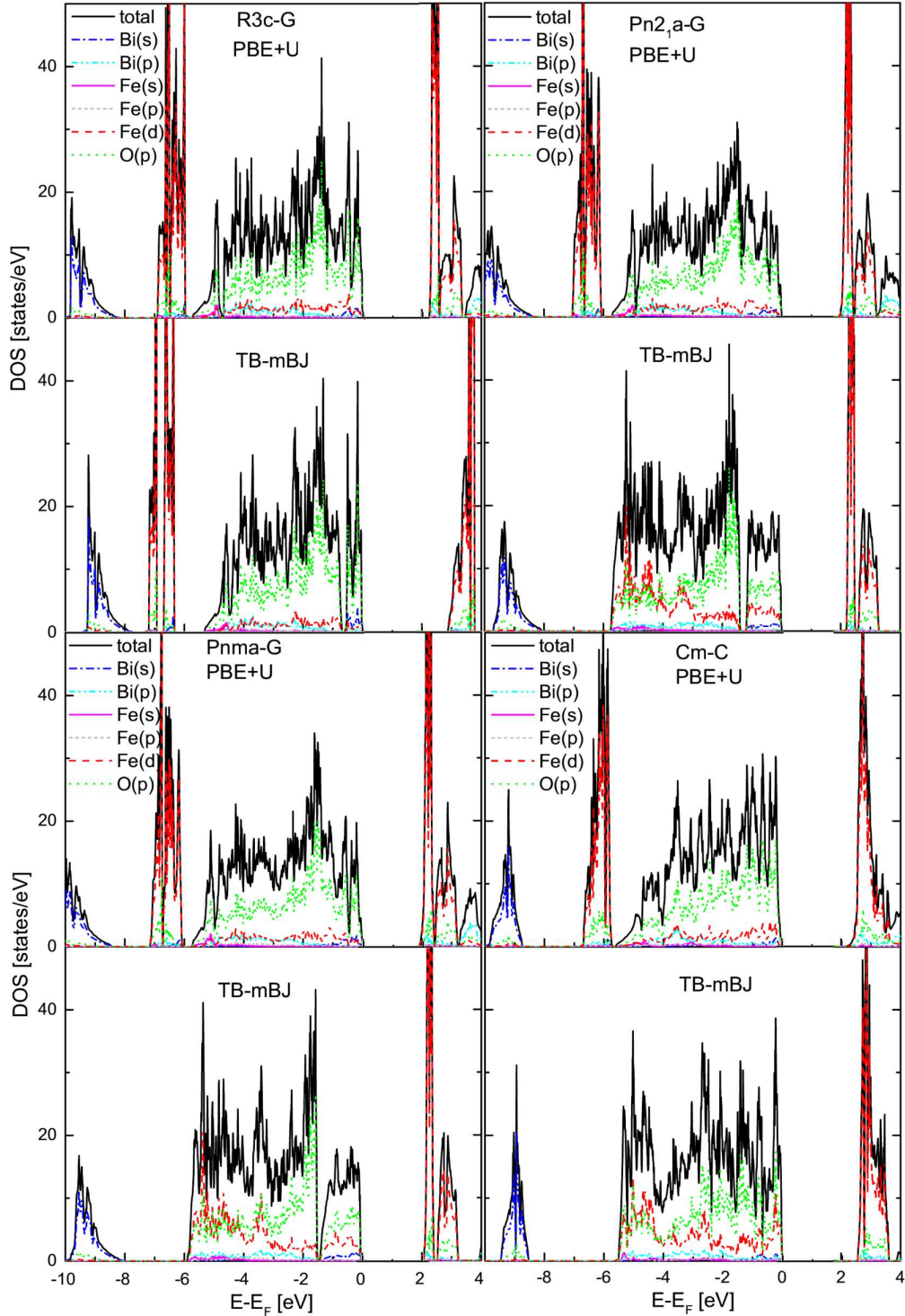


Fig. 1. Density of states of different phases of BiFeO_3 calculated within both PBE+ U (upper part) and TB-mBJ. For the AFM phases the results for spin-up and spin-down channel are the same.

In Fig. 1 we present the total and partial density of states (DOS) of aforementioned phases of BiFeO₃ calculated within PBE+*U* (upper part) and the semilocal TB-mBJ. In all cases the valence band (VB) is dominated by O 2*p* states with some contribution from Bi 6*p* and Fe 3*d* states (from -6 eV to 0 eV). The main difference in DOS between PBE+*U* and TB-mBJ results appears in the middle part of the VB (-6 eV to -8 eV) and connects with the Fe 3*d* orbitals. In PBE+*U* approach this region is dominated by the strongly localized Fe 3*d* for all structures and only for *R3c* within TB-mBJ. For other structures within TB-mBJ the Fe 3*d* states are shifted to higher energies and blur along the VB. This leads to the separation of the bands near the Fermi level. Similar behaviour has been observed in case of *d*-states in CaCuO₂ [10] and NiO [17]. The lower part of the valence band consists of Bi 6*s* state with some admixture of O 2*p* states (around -9 eV). The differences in DOS observed in unoccupied states for PBE+*U* and TB-mBJ calculations are associated with exact peak positions and relative intensities. The correctness of expectation of this part of DOS for applied approaches may be verified using experimental electron energy loss spectra. The conduction band is characterized mainly by the empty Fe 3*d* states with admixture of Bi 6*p* and O 2*p* states. The Bi 6*s* and O 2*p* orbitals in the lower part the VB and near the Fermi level form a pair of occupied bonding and anti-bonding states, respectively. The contribution from Bi 6*s* states near the top of the VB increases within TB-mBJ functional. Such situation is typical in the formation of lone pairs [18].

In Table II the band gaps (E_g) and Fe magnetic moments (μ_{Fe}) are given. The band gaps obtained within both approximation are rather similar. For *R3c-G* structure the value of the gap (2.26 eV) is comparable with experimental measurement determined from the UV-visible diffuse reflectance spectrum (2.5 eV) [19]. Both applied approaches give comparable values of magnetic moments on Fe.

TABLE II

Calculated band gaps (eV) and Fe magnetic moments (μ_B) for different phases of BiFeO₃.

Space group	E_g [eV]		μ_{Fe} [μ_B]	
	PBE+ <i>U</i>	TB-mBJ	PBE+ <i>U</i>	TB-mBJ
<i>R3c-G</i>	2.26	2.27	±4.11	±4.24
<i>Pnma-G</i>	1.91	1.66	±4.12	±4.03
<i>Pn2₁a-G</i>	1.99	2.18	±4.11	±4.03
<i>Cm-C</i>	2.09	2.55	±4.09	±4.00

4. Conclusions

The electronic structure of different phases of BiFeO₃ within PBE+*U* and TB-mBJ approaches were presented. The most stable phase is *R3c-G*. The band gaps within both approximations are similar and the calculated value of band gap for *R3c* phase is comparable to the experimental gap from the optical absorption spectra. Our cal-

culations suggested that TB-mBJ functional gives satisfactory results for the band gaps and the magnetic moments on Fe in BiFeO₃.

Acknowledgments

This work was supported by the National Science Centre (Poland) through Grant no. DEC-2011/01/B/ST3/02212.

References

- [1] G. Catalan, J.F. Scott, *Adv. Mater.* **21**, 2463 (2009).
- [2] M.M. Kumar, S. Srinath, G.S. Kumar, S.V. Suryanarayana, *J. Magn. Magn. Mater.* **188**, 203 (1998).
- [3] Yu.F. Popov, A.K. Zvezdin, G.P. Vorob'ev, A.M. Kadomtseva, V.A. Murashev, D.N. Rakov, *JETP Lett.* **57**, 69 (1993).
- [4] Y.J. Wu, K.X. Chen, J. Zhang, J.X. Chen, *J. Magn. Magn. Mater.* **324**, 1348 (2012); L. Luo, W. Wei, X. Yuan, K. Shen, M. Xu, Q. Xu, *J. Alloys Comp.* **540**, 36 (2012).
- [5] V. Khomchenko, V. Shvartsman, P. Borisov, W. Kleemann, D. Kiselev, I. Bdikin, J. Vieira, A. Kholkin, *Acta Mater.* **57**, 5137 (2009).
- [6] A.A. Belik, D.A. Rusakov, T. Furubayashi, E. Takayama-Muromachi, *Chem. Mater.* **24**, 3056 (2012); J. Yan, M. Gomi, T. Yokota, H. Song, *Appl. Phys. Lett.* **102**, 222906 (2013).
- [7] O. Diéguez, O.E. González-Vázquez, J.C. Wojdół, J. Íñiguez, *Phys. Rev. B* **83**, 094105 (2011).
- [8] S.L. Dudarev, G.A. Botton, S.Y. Savrasov, C.J. Humphreys, A.P. Sutton, *Phys. Rev. B* **57**, 1505 (1998).
- [9] F. Tran, P. Blaha, *Phys. Rev. Lett.* **102**, 226401 (2009).
- [10] D.J. Singh, *Phys. Rev. B* **82**, 205102 (2010).
- [11] D. Koller, F. Tran, P. Blaha, *Phys. Rev. B* **83**, 195134 (2011); H. Dixit, R. Saniz, S. Cottenier, D. Lamoen, B. Partoens, *J. Phys. Condens. Matter* **24**, 205503 (2012).
- [12] A.P. Gaiduk, V.N. Staroverov, *J. Chem. Phys.* **131**, 044107 (2009).
- [13] P.E. Blöchl, *Phys. Rev. B* **50**, 17953 (1994); G. Kresse, D. Joubert, *Phys. Rev. B* **59**, 1758 (1999).
- [14] G. Kresse, J. Furthmüller, *Phys. Rev. B* **54**, 11169 (1996).
- [15] J.P. Perdew, K. Burke, M. Ernzerhof, *Phys. Rev. Lett.* **77**, 3865 (1996).
- [16] M. Pugaczowa-Michalska, J. Kaczkowski, A. Jezierski, *Ferroelectrics* **461**, 85 (2014).
- [17] W. Hetaba, P. Blaha, F. Tran, P. Schattschneider, *Phys. Rev. B* **85**, 205108 (2012).
- [18] A. Walsh, D.J. Payne, R.G. Egdell, G.W. Watson, *Chem. Soc. Rev.* **40**, 4455 (2011).
- [19] F. Gao, Y. Yuan, K.F. Wang, X.Y. Chen, F. Chen, J.-M. Liu, Z.F. Ren, *Appl. Phys. Lett.* **89**, 102506 (2006).